

Structure of the Super Neutronised Doubly Closed Shell Nucleus ^{132}Sn

Rupayan Bhattacharya

Department of Physics, University of Botswana,
Private Bag 0022, Gaborone, Botswana.

Abstract

The scenario of single particle (proton as well as neutron) states near the Fermi surface of ^{132}Sn has been investigated on the basis of an average one-body potential suitably optimised for ^{208}Pb and then extrapolated to the mass region concerned. The calculation shows excellent agreement with experiment. The ground state charge distribution of the nucleus has also been calculated.

1. Introduction

The doubly magic nuclei and their immediate neighbours are of particular interest to nuclear structure physicists since they allow the most stringent tests of the shell model. Of all the doubly magic nuclei, ^{132}Sn with 50 protons and 82 neutrons, is the least accessible to experiment due to its very short half-life (40 s). The behaviour of this doubly closed shell nucleus which has a large N/Z ratio has created much interest in recent times both from experimentalists as well as theoreticians.

The magic behaviour of any nucleus emerges from its single (quasi) particle spectrum near the Fermi surface. The signature for strong shell closure comes out of the excitation spectrum of the nucleus concerned. Since these states are based on particle-hole excitation, their values give an indication of the proton or neutron shell gap. Another important characteristic peculiar to a magic nucleus is the absence of superfluid pair correlations. These correlations vanish because of the presence of a sufficiently wide energy gap between the fully occupied and the vacant states, so that the interaction forces in the particle-particle channel with $J = 0^+$ are not strong enough to transfer pairs into the vacant states.

2. Experimental Evidence

The initial indication of ^{132}Sn playing the role of a good closed core came from the work by Kerek *et al.* (1972, 1973) who investigated the ground state properties of ^{132}Sn and its neighbours. In another work Aleklett *et al.* (1977) studied the nucleus ^{132}Sn and its neighbours from the point of view of the shape of the mass surface in the region far away from the β -stability line. Mass data

on extremely neutron rich nuclei are important for theories of nucleosynthesis (Cameron *et al.* 1970) and also for predictions on superheavy elements (Nix 1970). Studies of level schemes of nuclei having one particle (proton or neutron) outside the core reveal the shell model properties of the nucleus. In this respect studies of the low lying excitation spectrum of ^{133}Sn (Sistemich *et al.* 1978) and ^{133}Sb (Borg *et al.* 1973) clearly show that ^{132}Sn can be taken as a good vibrator. Similarly, the structure of the neutron-hole nucleus ^{131}Sn , as studied by De Geer and Holm (1980), brings out the states which can be explained on the basis of ($^{132}\text{Sn}, n^{-1}$) coupling. These assignments are based on systematic studies of lighter odd mass Sn isotopes. The identification of the complete set of single hole levels in ^{131}Sn has been reported by Fogelberg and Blomqvist (1984). However, the main difficulty in identifying single particle and single hole levels in this region is due to a lack of stripping and pick-up reaction data.

The level scheme of ^{132}Sn has been studied with the on-line isotope separators for fission products in OSIRIS (Kerek *et al.* 1972), JOSEF (Lauppe *et al.* 1978) and ISOLDE (Bjornstad *et al.* 1982). In all these investigations the lowest lying excited state of ^{132}Sn was observed at 4.041 MeV. This shows that the shell closure is somewhat more pronounced in this nucleus compared with other doubly closed shell nuclei (for example the first excited 3^{-} state of ^{208}Pb lies at 2.614 MeV).

3. Theoretical Work

A structure calculation for the doubly magic nucleus ^{132}Sn by Dehesa and Speth (1978) was done within the RPA formalism and compared with the experimental results. Severe uncertainties were introduced into the calculation due to the lack of experimental data. As the single particle transfer data are absent here, the single particle wavefunctions and energy values were taken from a Woods-Saxon potential adjusted to ^{132}Sn . The most important result in this type of calculation is the energy gap between the particle and hole states.

A similar type of RPA calculation for ^{132}Sn was done by Conci and Klemt (1980) using a generalised particle-hole interaction which included, in addition to the zero range terms of the Landau-Migdal interaction, the explicit contributions of the one-pion and one-boson exchange potentials. After modification of the interpolation radii they could reproduce the level scheme of ^{132}Sn satisfactorily.

The single particle (hole) levels of ^{132}Sn have been reported on the basis of the independent particle model and mean-field theory by Leander *et al.* (1984). However, there the emphasis was only on the reproduction of single particle levels in different regions of magicity. Whether there is some correlation in the formation of clusters around a specific N or Z number with an increase of valence nucleon number is not apparent. We, therefore, have undertaken a critical study of the situation where an average one-body potential with smooth geometry is able to depict the islands of stability throughout the nuclear chart. The mass range from 140 to 220 was analysed by Mukherjee *et al.* (1981), where a proton magic gap of 2.3 MeV at $Z = 64$ and a neutron magic gap of 4.5 MeV at $N = 82$ were established. In the present work we show that for the mass $A = 132$ the method works well in bringing out the shell gap. Application of the same procedure has been found to be very effective for the mass range 40–50 (Krishan and Bhattacharya 1992).

4. Present Work

Because of the interplay of the neutron–proton interaction it is well known that the shell gap at $N = 126$ disappears as we move up the periodic table. In our search for the bunching effect of the single particle energy levels around the $A = 130\text{--}140$ region, evaluation of the energy levels was pivoted around a good set of potential parameters which can be used for most of the magic nuclei and their neighbours. The magic gap at $Z = 50$ and $N = 82$ depends crucially on the $1g_{7/2}$ proton state and $1h_{9/2}$ neutron state in ^{208}Pb and the variation of the binding energies with decreasing mass number. Thus, a critical choice is necessary of a set of realistic potential parameters in ^{208}Pb after taking core polarisation corrections into account and then a suitable extrapolation formula. This is imperative as the dynamical fragmentation of shell model states is well understood for ^{208}Pb and all the zeroth order shell model states are known. The justification for our model can be found in the calculated value of the shell gap in another doubly magic nucleus ^{146}Gd (Mukherjee *et al.* 1981). The confidence obtained there led us to explore another area of magicity.

Table 1. Woods–Saxon potential parameters for ^{208}Pb

	V_0	r_0	a_0	V_s	r_s	a_s
Neutron	42.479	1.310	0.718	24.312	1.246	0.391
Proton	64.620	1.184	0.640	32.510	1.136	0.785

Table 2. Single particle neutron and proton states of ^{208}Pb

Neutron states	Neutron binding energy (MeV)		Proton states	Proton binding energy (MeV)	
	Theory	Expt		Theory	Expt
$3d_{3/2}$	1.32	1.42	$3p_{1/2}$		Unbound
$2g_{7/2}$	1.35	1.45	$3p_{3/2}$		0.04
$4s_{1/2}$	1.64	1.91	$2f_{5/2}$		0.33
$1j_{15/2}$	2.35	1.95	$1i_{13/2}$	1.55	1.70
$3d_{5/2}$	2.17	2.36	$2f_{7/2}$	2.46	2.30
$1i_{11/2}$	3.37	3.15	$1h_{9/2}$	3.50	3.60
$2g_{9/2}$	4.01	3.74	$2s_{1/2}$	7.71	8.03
$3p_{1/2}$	7.52	7.38	$2d_{3/2}$	8.37	8.38
$2f_{5/2}$	8.14	7.95	$1h_{11/2}$	9.14	9.37
$3p_{3/2}$	8.33	8.27	$2d_{5/2}$	10.18	10.23
$1i_{13/2}$	8.65	9.38	$1g_{7/2}$	11.99	12.03
$2f_{7/2}$	10.41	10.38	$1g_{9/2}$	16.15	16.03
$1h_{9/2}$	10.88	11.28			
$1h_{11/2}$	14.62	14.50			

In Table 1 we present the optimised Woods–Saxon potential parameters for the nucleus ^{208}Pb , which reproduce the single particle states of this nucleus after taking care of the core polarisation correction. In order to understand the fragmentation of the neutron states of ^{208}Pb it was shown in the work of Mukherjee *et al.* (1979) that the coupling of the shell model states of ^{208}Pb can

quantitatively account for the stripping and pickup reaction data. Each state is expanded as

$$|\alpha j\rangle = \sum_{j'} \alpha_{\lambda j'} |\lambda j', j\rangle,$$

where $\lambda + j' = j$ and $\lambda = 0^+, 3^-, 5^-, 2^+, 4^+$ and 6^+ . The core particle interaction is $H_{\text{int}} = k(r)(2\lambda + 1)^{1/2}(\alpha_\lambda Y_\lambda)_0$ (Bohr and Mottelson 1975), where $k(r) = 1/r(dV/dr)$ produces admixture of these states. The phonon energies $\hbar\omega_\lambda$ and the vibrational amplitudes $\langle \alpha_\lambda \rangle$ were taken from the experimental data. The observed spectroscopic factors are equated with a_{0j}^2 . The set of binding energies which are solutions of the secular equation are shown in Table 2. In finding the zeroth order single particle proton states of ^{208}Pb we have used the same method assuming that similar dynamics prevail. It has been found that this phenomenological approach to the core polarisation effect gives a better description of the experimental situation than the microscopic approach of Hamamoto and Siemens (1976). In order to examine the shell model states in the lower mass region our prescription is not to alter the geometry (which means an identical radius and diffuseness parameter where the radius of course has an $A^{1/3}$ dependence), but to change the depth of the potential according to the following equations:

$$V_n = \left(V_{0n} - K_n \frac{N - Z}{A} \right) f_n(r), \quad (1)$$

$$V_p = \left(V_{0p} - K_p \frac{N - Z}{A} \right) f_p(r). \quad (2)$$

It was found that for K_n and K_p separately adjusted to 33.0 MeV the prescription works well to reproduce the known neutron states in the $N = 82$ nuclei of Ce, Nd, and Sn and the proton states of the $Z = 50$ nucleus Sn. In Table 1 V_0 represents V_n and V_p for ^{208}Pb . Table 2 presents the single particle proton and neutron states of ^{208}Pb , as calculated by our potential along with the experimental states. The close correspondence between the theoretical and experimental levels indicates the reliability of the potential parameters. The spin-orbit strength was varied according to

$$V_s(^{132}\text{Sn}) = V_s(^{208}\text{Pb}) V_0(^{132}\text{Sn}) / V_0(^{208}\text{Pb}). \quad (3)$$

The single particle proton states of ^{132}Sn are shown in Table 3. The limitation set by the experiments led us to compare the calculated energy values for a few states only, e.g. $1f_{5/2}$, $1g_{7/2}$, $1g_{9/2}$, $2d_{5/2}$, $1h_{11/2}$, with the experimental values which are the centroids of observed states. This supports the appropriateness of our extrapolation constant and, at the same time, enhances the justification for our method of extracting the potential parameters starting from ^{208}Pb . The experimental value for the state $1f_{5/2}$ was provided by B. Fogelberg (personal communication 1990). In Table 3 we also present a comparison of the single particle neutron states near the Fermi surface of ^{132}Sn , obtained experimentally and theoretically.

Table 3. Single particle proton and neutron states of ^{132}Sn

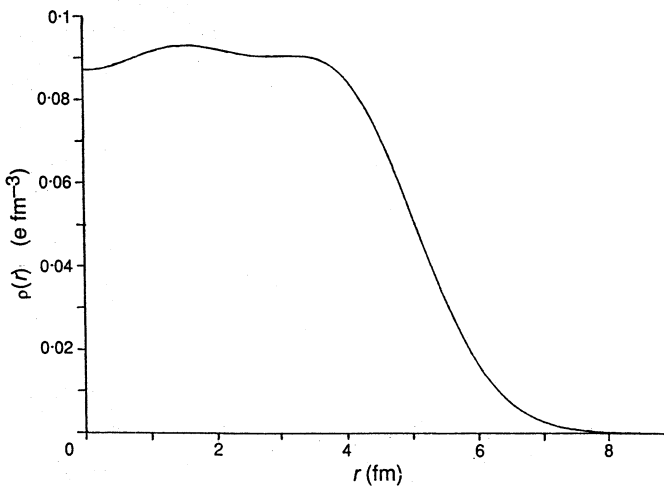
Proton states	Proton binding energy (MeV)		Neutron states	Neutron binding energy (MeV)	
	Theory	Expt		Theory	Expt
$1f_{7/2}$	23.05		$1g_{7/2}$	9.45	9.72
$1f_{5/2}$	19.00	18.97	$2d_{5/2}$	9.53	8.95
$2p_{3/2}$	17.77		$3s_{1/2}$	7.88	7.62
$2p_{1/2}$	16.36		$1h_{11/2}$	6.62	7.53
$1g_{9/2}$	14.80	15.38	$2d_{3/2}$	7.59	7.29
$1g_{7/2}$	8.99	9.68	$2f_{7/2}$	2.59	2.63
$2d_{5/2}$	8.66	8.72	$3p_{3/2}$	1.48	
$3s_{1/2}$	6.12		$3p_{1/2}$	1.00	
$2d_{3/2}$	6.17		$1h_{9/2}$	0.97	
$1h_{11/2}$	5.99	6.89			

Only in the case of the high spin proton state $1h_{11/2}$ do we find a discrepancy as large as 0.9 MeV; otherwise the agreement is good. As soon as the spectroscopic strengths for these states become available, our comparison will be much more meaningful. We have calculated the r.m.s. charge radii and valence nucleon orbit radii for even tin isotopes and obtained excellent agreement with experiment (Bhattacharya 1986). In the same spirit we have extended our program to ^{132}Sn and found values of $\langle r^2 \rangle^{1/2}$ of 4.548, 4.547 and 5.231 fm for the $2p_{3/2}$, $2p_{1/2}$ and $1g_{9/2}$ states respectively. In obtaining these values we calculated the charge distribution of the nucleus using the formula

$$\rho(r) = \sum (2j + 1) \psi_j^2(r), \quad (4)$$

where the sum is over all occupied levels and where $\psi_j(r)$ are the single particle proton levels below the Fermi surface. In calculating the charge distribution we have taken into account the c.m. correction, the finite proton size, etc., and we have also used the non-locality correction.

Fig. 1 shows our charge distribution which was used to calculate our r.m.s. charge radius of $\langle r^2 \rangle^{1/2} = 4.827$ fm. Table 4 shows the Fourier-Bessel coefficients

**Fig. 1.** Charge distribution for ^{132}Sn .

of the ground state charge distribution, calculated by the prescription

$$\rho(r) = \sum_{\mu} a_{\mu} j_0(q_{\mu} r), \quad r < R$$

$$= 0, \quad r > R,$$

with $q_{\mu} = \pi\mu/R$ and where R is the cutoff radius. Here $\rho(r)$ is normalised such that $4\pi \int \rho(r)r^2 dr = Ze$. In our calculation $R = 10.0$ fm and $\mu = 10$. Since there are no experimental data here we cannot compare our result.

Table 4. Fourier–Bessel coefficients for the charge distribution of ^{132}Sn

μ	a_{μ}	μ	a_{μ}
1	0.0662	6	0.0226
2	0.0765	7	-0.0080
3	-0.0341	8	-0.0105
4	-0.0461	9	-0.0010
5	0.0204	10	0.0010

5. Conclusions

In this work we have reproduced the single particle structure of the doubly magic nucleus ^{132}Sn . The cluster of single particle states in the mass region 100–150 can be obtained reliably if one starts with a one-body shell model potential that works for the Pb region. In our previous work (Bhattacharya 1986) we showed that for even isotopes of tin ($A = 112$ –24) our method reproduces well the valence orbit radii and total r.m.s. charge radii along with the energies of the valence proton states. Thus, we find a correlation among the islands of magicity. Future reaction data should testify to the utility of this calculation.

Acknowledgment

The author acknowledges with thanks the good advices of the respected referee for the betterment of the paper.

References

- Aleklett, K., Lund, E., and Rudstam, G. (1977). *Nucl. Phys. A* **281**, 213; **286**, 403.
 Bhattacharya, R. (1986). *Phys. Rev. C* **33**, 2185.
 Bjornstad, R., *et al.* (1982). *Z. Phys. A* **306**, 951.
 Bohr, A., and Mottelson, B. R. (1975). ‘Nuclear Structure’, Vol. II (Benjamin: Massachusetts).
 Borg, S., Holm, G. B., and Rydberg, B. (1973). *Nucl. Phys. A* **212**, 197.
 Cameron, A. G. W., Delane, M. O., and Truran, J. M. (1970). Proc. 2nd Int. Conf. on Nuclei Far from Stability, Leysin (CERN 70-30), p. 753.
 Conci, G., and Klemt, V. (1980). Jülich Kern Physik Annual Rep., p. 86.
 De Geer, L. E., and Holm, G. B. (1980). *Phys. Rev. C* **22**, 2163.
 Dehesa, J. S., and Speth, J. (1978). *Phys. Lett. B* **73**, 309.
 Fogelberg, B., and Blomqvist, J. (1984). *Phys. Lett. B* **137**, 20.
 Hamamoto, I., and Siemens, P. (1976). *Nucl. Phys. A* **269**, 199.
 Kerek, A., Holm, G. B., Carlé, P., and McDonald, J. (1972). *Nucl. Phys. A* **195**, 159, 177; **198**, 466.
 Kerek, A., Holm, G. B., De Geer, L. E., and Borg, S. (1973). *Phys. Lett. B* **44**, 252.

- Krishan, K., and Bhattacharya, R. (1992). *Phys. Rev.* (to be published).
- Lauppe, W. D., *et al.* (1978). *J. Phys. Soc. Jpn* **44**, 335.
- Leander, G. A., *et al.* (1984). *Phys. Rev. C* **30**, 416.
- Mukherjee, P., Bhattacharya, R., and Mukherjee, I. (1981). *Phys. Rev. C* **24**, 1810.
- Mukherjee, P., Majumder, R., and Mukherjee, I. (1979). *Phys. Rev. C* **19**, 562.
- Nix, J. R. (1970). Proc. 2nd Int. Conf. on Nuclei Far from Stability, Leysin (CERN 70-30), p. 735.
- Sistemich, J., *et al.* (1978). *Z. Phys. A* **285**, 305.

Manuscript received 1 October 1990, accepted 12 September 1991

